Journal of Molecular Structure 1147 (2017) 438–451

Contents lists available at ScienceDirect

Journal of Molecular Structure

journal homepage: http://www.elsevier.com/locate/molstruc

Structural variety in copper(II) complexes of 3-formylchromone: Synthesis, spectral, thermal, molecular modeling and biological studies

Magdy Shebl*, Omima M.I. Adly, A. Taha, N.N. Elabd

Department of Chemistry, Faculty of Education, Ain Shams University, Roxy, Cairo, Egypt

ARTICLE INFO

Article history:
Received 15 January 2017
Received in revised form
17 June 2017
Accepted 19 June 2017
Available online 21 June 2017

Keywords:
Binary and ternary complexes
3-Formylchromone
ESR spectra
Molecular modeling
Antimicrobial activity

ABSTRACT

The compound in the title (L) was synthesized and reacted with Cu(II) metal ion with different anions (OAc^-, NO_3^-, SO_4^{2-}, ClO_4^-, Cl^- and Br^-) in absence and presence of auxiliary ligands (L′); N,O-donor; or N,N-donor; to form binary and ternary Cu(II)-chelates. The metal complexes were fully characterized by analytical and spectral techniques in addition to thermal, conductivity and magnetic susceptibility measurements. The obtained results showed that the ligand behaves as a neutral bidentate, forming chelates with molar ratios: 1:1, 1:2 and 1:3; M:L for binary and 1:2:1 and 1:1:1; M:L:L′ for ternary complexes, which can be formulated as: $[L_mCuX_n(H_2O)_y]\cdot zH_2O$, m = 1 or 2, n = 0, 1 or 2, X = OAc^-, SO_4^{2-}, Cl^- or Br^-, y = 0 or 2, z = 0 or 0.5; $[L_mCu(H_2O)_n]X_2\cdot zMeOH$, m = 2 or 3, n = 0 or 2, X = ClO_4^- or NO_3^-, z = 0 or 1 and $[L_m\,L'Cu(H_2O)_n](NO_3)_x\cdot yS$, m = 1 or 2, n = 0 or 2, X = 1 or 2, y = 0.5 or 4, S = H_2O or MeOH. The ESR spin Hamiltonian parameters of some complexes were calculated. Kinetic parameters (Ea, A, ΔH, ΔS and ΔG) of the thermal decomposition stages have been evaluated using Coats–Redfern equations. The structural parameters of the ligand and its metal complexes have been calculated and correlated with the experimental data. The metal complexes exhibited octahedral and square planar geometrical arrangements according to the nature of the anion. The ligand and its metal complexes showed antibacterial activity towards Gram–positive bacteria, Gram–negative bacteria, yeast and fungus.

1. Introduction

The benzopyron ring system is fundamental in essential classes of bioactive natural products as coumarines, chromones and flavonoids. Chromones are the most widespread class of naturally occurring compounds. Chromones have potential beneficial effects for human health [1,2]. Among the diverse biological properties [3] that these compounds possess are included activities like anti-inflammatory [4], antibacterial [5], antitumor [6,7], antioxidant [4,6,7], anti-HIV [8], vasodilator, antiviral and antiallergenic activities [6,7]. 3-Formylchromone and its substituents have attracted a considerable interest as highly reactive compounds, which can form the metal-heterocyclic complexes with useful properties due to the availability of oxygen as a donor center.

Copper(II) ion plays vital roles in various biological processes such as its role in the action of different enzymes that catalyze a great variety of reactions. Copper(II) complexes have attracted a significant interest as a result of their biological and pharmaceutical properties [9]. Furthermore, it has been reported that the presence of a nitrogen donor heterocyclic ligand, such as 1,10-phenanthroline or 2,2′-bipyridine and so on [10] improves the biological activity of copper(II) complexes.

The object of the present work is to study the chelating behavior of 3-formylchromone (4-oxo-4H-1-benzopyran-3-carboxal dehyde); Scheme 1; towards copper(II) ion. We are interested to study the effect of anions on the structure of the prepared complexes, which may serve in different fields. Thus, a series of binary and ternary copper(II) complexes have been synthesized by using copper(II) ion with different anions (AcO^-, NO_3^-, SO_4^{2-}, ClO_4^-, Cl^- and Br^-) and auxiliary ligands (Scheme 1) including N,O-donor; 8-hydroxyquinoline or N,N-donor; 1,10-phenanthroline and 2,2'-bipyridyl. The prepared complexes have been characterized by micro analytical, spectral (IR, electronic, ESR and mass spectra), thermal, magnetic and conductivity techniques. Molecular modeling was carried out for the free ligand and its copper(II) chelates and the theoretical results were correlated with the

* Corresponding author.
E-mail address: magdy_shebl@hotmail.com (M. Shebl).

http://dx.doi.org/10.1016/j.molstruc.2017.06.085
0022-2860/

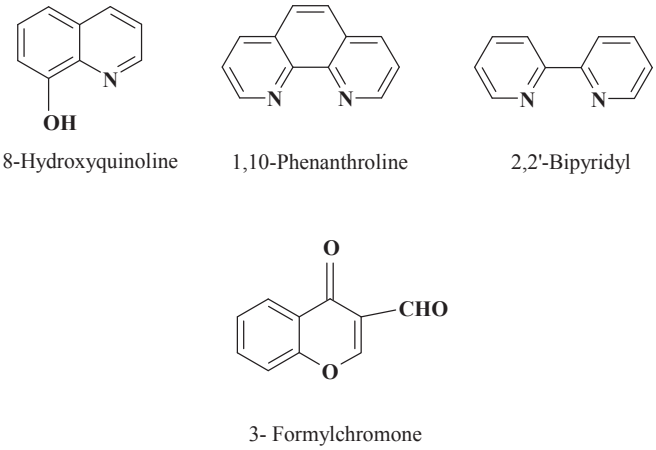

Scheme 1. Structures of the primary ligand; 3-formylchromone and auxiliary ligands; 8-hydroxyquinoline, 1,10-phenanthroline and 2,2'-bipyridyl.

experimental data. The antimicrobial activity of the ligand and its complexes was examined against Gram−positive bacteria (*Staphylococcus aureus* and *Bacillus subtilis*), Gram−negative bacteria (*Salmonella typhimurium* and *Escherichia coli*), yeast (*Candida albicans*) and fungus (*Aspergillus fumigatus*).

2. Experimental

2.1. Measurements

Elemental analyses (C, H, N and S) were carried out by means of Vario El-Elementar at the Ministry of Defense, Chemical War Department. Analysis of the copper(II) ion followed the decomposition of an accurate weight of the solid complex with concentrated HNO_3, neutralizing with ammonia and titrating with EDTA. Decomposition temperatures of the complexes were determined using a Stuart SMP3 melting point apparatus. IR spectra were recorded as KBr discs on FT IR Nicolet IS10 spectrometer. Electronic spectra were recorded on a Jasco model V-550 UV/Vis spectrophotometer as Nujol mulls and/or solutions in DMF. ESR spectra were recorded at Elexsys, E500, Bruker company. 2,2′-Diphenyl-1-picrylhydrazyl (DPPH) was employed to calibrate the magnetic field. Mass spectra were recorded on GC-2010 Shimadzu Gas chromatography instrument mass spectrometer. Samples were introduced directly to the probe and the fragmentations were performed at 300 °C and 70 eV. The magnetic susceptibility measurements were carried out at room temperature using a magnetic susceptibility balance of the type Johnson Matthey, Alfa product, Model No. (MKI). Effective magnetic moments were calculated and corrected using Pascal's constants for the diamagnetism of all atoms in the compounds [11]. Molar conductivity measurements of 10^{-3} M solutions of the solid complexes in DMF were measured on the Corning conductivity meter NY 14831 model 441. TGA-measurements were carried out from room temperature up to 800 °C at a heating rate of 10 °C/min on a Shimadzu-50 thermal analyzer. The biological activity of the ligand and its metal complexes was studied using the disc diffusion method.

2.2. Materials

3-Formylchromone was prepared according to literature method [12]. Metal salts, 8-hydroxyquinoline, 1,10-phenanthroline, 2,2'-bipyridyl, EDTA disodium salt, ammonium hydroxide, mureoxide and nitric acid were either Merck, Aldrich or BDH products. Organic solvents were reagent grade chemicals and were used without distillation.

Caution! As perchlorate salts of metal ions are potentially explosive especially in the presence of organic ligands, only a small amount should be prepared and handled with intensive care.

2.3. Synthesis of the metal complexes

As representative examples, the following synthetic methods are provided in details and the other complexes are obtained similarly.

2.3.1. Synthesis of $[(L)_2Cu(OAc)_2]\cdot 0.5H_2O$, **1**

0.5 g (2.87 mmol) of the ligand, L, was dissolved in 30 ml hot methanol. To this hot ligand solution, 30 ml methanolic solution of 0.572 g (2.87 mmol) of $Cu(OAc)_2\cdot H_2O$ was added drop by drop with continuous stirring. The reaction mixture was heated under reflux for 8 h, which resulted a deep green precipitate. The deep green solid was separated out after cooling at room temperature, filtered, washed with methanol and dried at room temperature; the precentage yield was 70%. The complex was kept in a desiccator over anhydrous calcium chloride.

2.3.2. Synthesis of $[(L)_2Cu(8\text{-}HQ)]NO_3\cdot MeOH$, **7**

0.5 g (2.87 mmol) of the ligand, L, was dissolved in 30 ml hot methanol. To this hot ligand solution, 30 ml methanolic solution of 0.667 g (2.87 mmol) of $Cu(NO_3)_2.2.5H_2O$ was added drop by drop with continuous stirring. The reaction mixture was heated under reflux for 30 min and then 0.417 g (2.87 mmol) of 8-hydroxyquinoline (8-HQ) dissolved in methanol was added to the above mixture. The resultant mixture was heated under reflux for 8 h, which resulted a deep cumin green precipitate. The complex was allowed to cool at room temperature. The solid product was filtered, washed with methanol and dried at room temperature; the precentage yield was 91%. The complex was kept in a desiccator over anhydrous calcium chloride.

2.3.3. Unsuccessful trials

Trials to prepare the ternary Cu(II) complex of the ligand in the presence of glycine were unsuccessful where the binary complex was obtained.

2.4. Molecular modeling

In an attempt to gain a superior insight on the molecular structure of the chelating agent and its complexes, geometrical optimization and conformation analysis have been performed using PM3 forcefield as implemented in hyperchem 7.5 [13].

2.5. Antimicrobial activity

The biological activity of the synthesized compounds was investigated according to the standardized disc-agar diffusion technique [14,15]. The organisms include *Staphylococcus aureus* (ATCC 25923) and *Bacillus subtilis* (ATCC 6635) as Gram positive bacteria, *Salmonella typhimurium* (ATCC 14028) and *Escherichia coli* (ATCC 25922) as Gram negative bacteria and *Candida albicans* (ATCC 10231) and *Aspergillus fumigatus* as fungus strain. The antibiotics chloramphenicol and cephalothin were used as reference in case of Gram-positive bacteria and Gram-negative bacteria, respectively while the refernce was cycloheximide in case of fungi.

2.5.1. Preparation of the tested compound

The tested compounds were dissolved in dimethylformamide and prepared in two concentrations; 100 and 50 mg/ml and after

Table 1
Analytical and physical data of the copper(II) complexes.

No.	Reaction	Complex M. F. [F. Wt]	Color	Yield (%)	M.P. °C	Elemental analysis, % Found/(Calc.)			
						C	H	N/S	M
(1)	L + $Cu(OAc)_2·H_2O$	$[(L)_2Cu(OAc)_2]·0.5H_2O$ $C_{24}H_{19}O_{10.5}Cu$ [538.96]	Deep green	70	226	53.1 (53.49)	3.96 (3.55)	–	11.6 (11.79)
(2)	L + $Cu(NO_3)_2·2.5H_2O$	$[(L)_3Cu](NO_3)_2·MeOH$ $C_{31}H_{22}N_2O_{16}Cu$ [742.07]	Green	30	200	50.3 (50.18)	3.2 (2.99)	3.6 (3.78)	8.4 (8.56)
(3)	L + $CuSO_4·5H_2O$	$[(L)Cu(SO_4)(H_2O)_2]$ $C_{10}H_{10}O_9SCu$ [369.8]	Green	30	226	32.7 (32.48)	2.5 (2.73)	8.5 (8.67)	17.00 (17.18)
(4)	L + $Cu(ClO_4)_2·6H_2O$	$[(L)_2Cu(H_2O)_2](ClO_4)_2$ $C_{20}H_{16}O_{16}Cl_2Cu$ [646.79]	Pale green	26	a	37.48 (37.14)	2.1 (2.49)	–	a (9.82)
(5)	L+ $CuCl_2·2H_2O$	$[(L)CuCl_2(H_2O)_2]·0.5H_2O$[b] $C_{10}H_{11}O_{5.5}Cl_2Cu$ [353.65]	Pale green	30	>300	33.7 (33.96)	3.50 (3.14)	–	17.8 (17.97)
(6)	L+ $CuBr_2$	$[(L)CuBr_2)]·0.5H_2O$ $C_{10}H_7O_{3.5}Br_2Cu$ [406.52]	Green	31	265	29.3 (29.55)	1.79 (1.74)	–	15.5 (15.63)
(7)	L+ $Cu(NO_3)_2·2.5H_2O$ + 8-HQ	$[(L)_2Cu(8\text{-HQ})]NO_3·0.5MeOH$ $C_{29.5}H_{20}N_2O_{10.5}Cu$ [634.04]	Deep cumin green	91	>300	56.5 (56.24)	3.22 (3.2)	4.7 (4.45)	10.0 (10.09)
(8)	L+ $Cu(NO_3)_2·2.5H_2O$ + Phen	$[(L)Cu(Phen)(H_2O)_2](NO_3)_2·4H_2O$ $C_{22}H_{26}N_4O_{15}Cu$ [650.02]	Pale blue	25	264	40.63 (40.65)	3.8 (4.03)	8.9 (8.62)	9.6 (9.78)
(9)	L+ $Cu(NO_3)_2·2.5H_2O$ + Bipy	$[(L)_2Cu(Bipy)](NO_3)_2·0.5H_2O$ $C_{30}H_{21}N_4O_{12.5}Cu$ [701.07]	Green	22	210	51.1 (51.4)	3.4 (3.02)	8.2 (7.99)	8.9 (9.06)

[a] Not determined.
[b] The same complex was obtained by using copper(I) salt.

that 10 μl of each sample was dropped on disk of 6 mm in diameter and the concentrations became 1 and 0.5 mg/disk, respectively. Insoluble compounds were suspended in DMF and vortexed then processed.

2.5.2. Testing for anti-bacterial and yeasts activity

Bacterial cultures were grown in nutrient broth medium at 30 °C. After 16 h of growth, each microorganism, at a concentration of 10^8 cells/ml, was inoculated on the surface of Mueller-Hinton agar plates using sterile cotton swab. Subsequently, uniform size filter paper disks (6 mm in diameter) were impregnated by equal volume (10 μl) from the specific concentration of dissolved compounds and cautiously placed on surface of each inoculated plate. The plates were incubated in the upright position at 36 °C for 24 h. Three replicates were carried out for each extract against each of the test organism. At the same time, addition of the respective solvent instead of dissolved compound was carried out as negative controls. After incubation, the diameters of the growth inhibition zones formed around the disc were measured with transparent ruler in millimeter, averaged and the mean values were tabulated.

2.5.3. Testing for anti-fungal activity

Active inoculum for experiments was prepared by transferring many loopfuls of spores from the stock cultures to test tubes of sterile distilled water (SDW) that were agitated and diluted with sterile distilled water to attain optical density analogous to 2.0×10^5 spore/ml. Inoculum of 0.1% suspension was swabbed uniformly and the inoculum was allowed to dry for 5 min then the same procedure was followed as described above.

3. Results and discussion

The ligand reacted with several Cu(II) salts of AcO^-, NO_3^-, SO_4^{2-}, Cl^-, Br^- and ClO_4^- in order to study the effect of the counter ions on the products. Also, the ligand was allowed to react with copper(II) ion in the presence of auxiliary ligands (L′) [N,O-donor; 8-hydroxyquinoline or N,N-donor; 1,10-phenanthroline and 2,2'-bipyridyl]. The prepared complexes are stable at room temperature, non-hygroscopic and sparingly-soluble in water and common organic solvents. The obtained complexes are characterized by elemental and thermal analyses, IR, electronic, ESR and mass spectra as well as conductivity and magnetic moment measurements. The analytical data of the complexes are listed in Table 1.

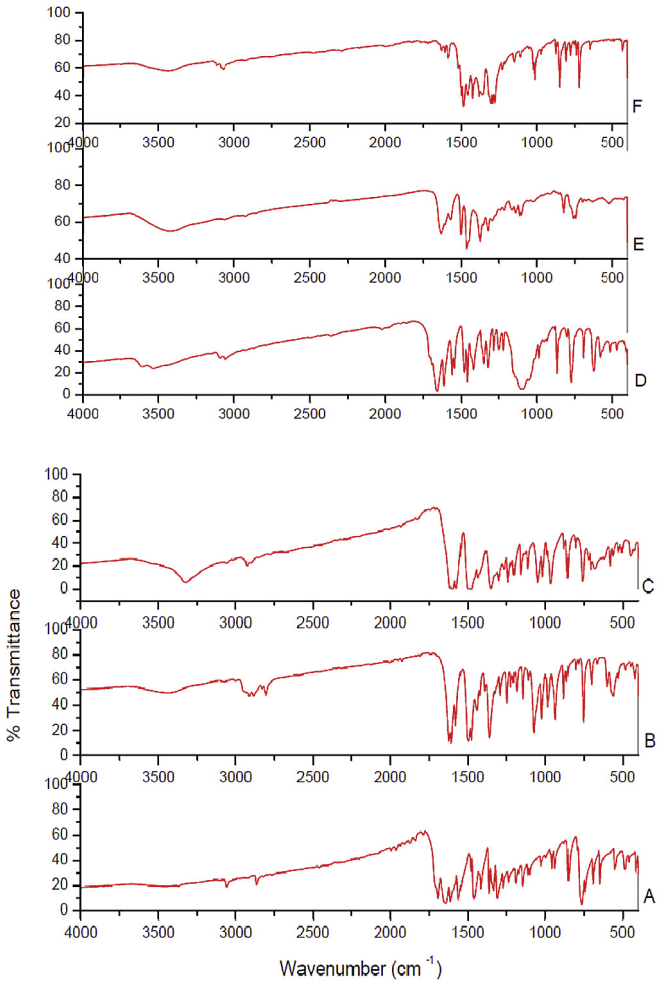

Fig. 1. IR spectra of the ligand (A), $[(L)_2Cu(OAc)_2]·0.5H_2O$ (B), $[(L)_3Cu](NO_3)_2·MeOH$ (C), $[(L)_2Cu(H_2O)_2](ClO_4)_2$ (D), $[(L)_2Cu(8\text{-HQ})]NO_3·0.5MeOH$ (E) and $[(L)Cu(Phen)(H_2O)_2](NO_3)_2·4H_2O$ (F).

Table 2
Characteristic IR spectral data of the ligand and its complexes.

No.	Complex	IR Spectra $(cm)^{-1}$					
		ν(OH)	ν(HC=O)	ν(C=O)	ν(M-O)	ν(M-N)	Other bands
	L	–	1694	1643	–	–	–
1	$[(L)_2Cu(OAc)_2]\cdot 0.5H_2O$	3422	1622	1606	538	–	1498 $\nu_{as}(COO^-)$, 1391 $\nu_s(COO^-)$; (monodentate OAc^-)
2	$[(L)_3Cu](NO_3)_2\cdot MeOH$	3321	1616	1598	525	470	1437; $\nu(NO_3^-)$ (ionic)
3	$[(L)Cu(SO_4)(H_2O)_2]$	3486	1637	1616	521	–	1069; $\nu(SO_4^{2-})$ (bidentate)
4	$[(L)_2Cu(H_2O)_2](ClO_4)_2$	3536	1660	1615	513	458	1092, 626; $\nu(ClO_4^-)$ (ionic)
5	$[(L)CuCl_2(H_2O)_2]\cdot 0.5H_2O$	3442	1618	1604	500	–	–
6	$[(L)CuBr_2)]\cdot 0.5H_2O$	3426	1616	1602	528	–	–
7	$[(L)_2Cu(8\text{-HQ})]NO_3\cdot 0.5MeOH$	3420	1634	1606	520	430	1375; $\nu(NO_3^-)$ (ionic), 1504; ν(C=N) 8-HQ
8	$[(L)Cu(Phen)(H_2O)_2](NO_3)_2\cdot 4H_2O$	3441	1630	1609	515	432	1427; $\nu(NO_3^-)$ (ionic), 1500; ν(C=N) Phen
9	$[(L)_2Cu(Bipy)](NO_3)_2\cdot 0.5H_2O$	3448	1623	1603	528	431	1424; $\nu(NO_3^-)$ (ionic)

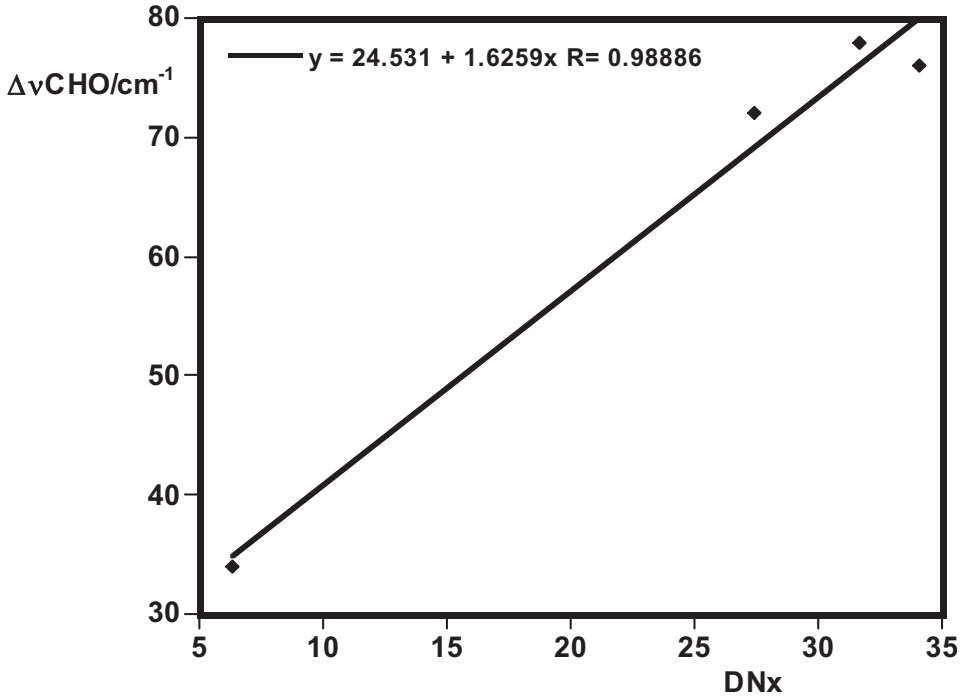

Fig. 2. Relationship between the bathochromic shift of νCHO versus the Lewis basicity of anions (DNx) taken from Ref. [31].

3.1. IR spectra

Fig. 1 shows the IR spectra of the ligand and some representative copper (II) complexes. Table 2 lists the characteristic IR spectral bands of the free ligand and its complexes. In order to determine the coordinating sites, the IR spectra of the complexes are compared with that of the ligand. The broad bands observed in the range 3321–3536 cm^{-1} can be assigned to ν(OH) of the coordinated or uncoordinated water molecules associated with the complexes. The presence of water molecules is verified by elemental and

Table 3
Electronic spectra, magnetic moments and molar conductivity data of the ligand and its complexes.

No.	Complex	Electronic spectral bands[a] (nm) λ_{max}[a] (nm)/(ε_{max} L cm^{-1} mol^{-1})	$\mu_{eff.}$ B.M.	Conductance[a] (Ω^{-1} cm^2 mol^{-1})
	L	271 (4340), 353 (4700), 387 (3415)	–	–
1	$[(L)_2Cu(OAc)_2]\cdot 0.5H_2O$	(423, 687)[b]	1.56	2.6
2	$[(L)_3Cu](NO_3)_2\cdot MeOH$	(636 sh)[b]	2.3	130
3	$[(L)Cu(SO_4)(H_2O)_2]$	(500, 686)[b]	2.15	1.5
4	$[(L)_2Cu(H_2O)_2](ClO_4)_2$	(495, 677)[c]	2.04	125
5	$[(L)CuCl_2(H_2O)_2]\cdot 0.5H_2O$	(500, 701)[c]	1.99	5.1
6	$[(L)CuBr_2)]\cdot 0.5H_2O$	(500, 695)[c]	2.15	2.3
7	$[(L)_2Cu(8\text{-HQ})]NO_3\cdot 0.5MeOH$	(448, 684)[b]	1.84	80
8	$[(L)Cu(Phen)(H_2O)_2](NO_3)_2\cdot 4H_2O$	(689)[b]	2.3	165
9	$[(L)_2Cu(Bipy)](NO_3)_2\cdot 0.5H_2O$	(615)[b]	2.03	140

[a] Solutions in DMF (10^{-3} M).
[b] Nujol mull.
[c] Concentrated solutions.

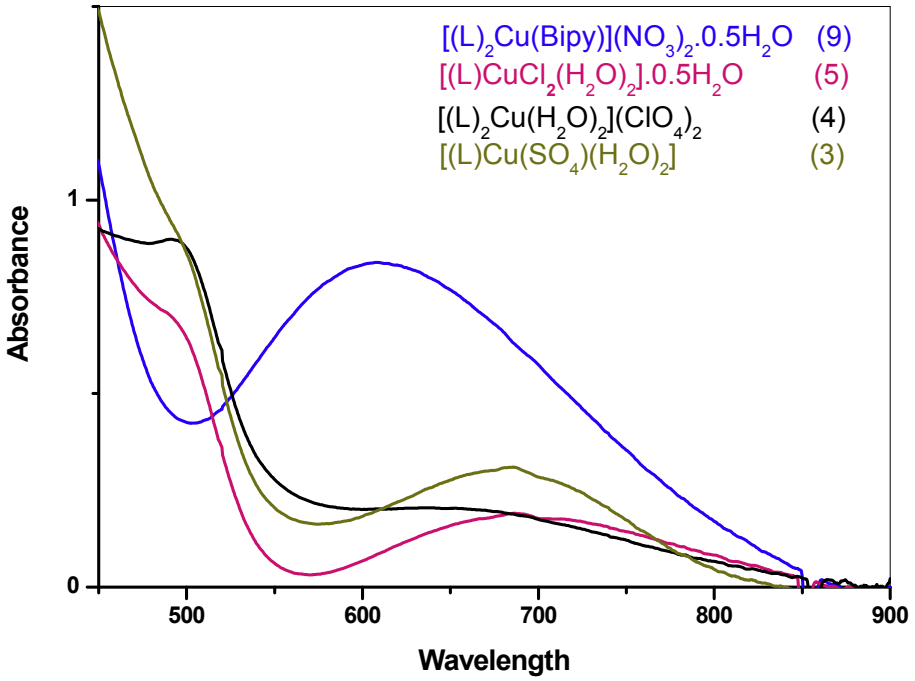

Fig. 3. Electronic spectra of some representative complexes.

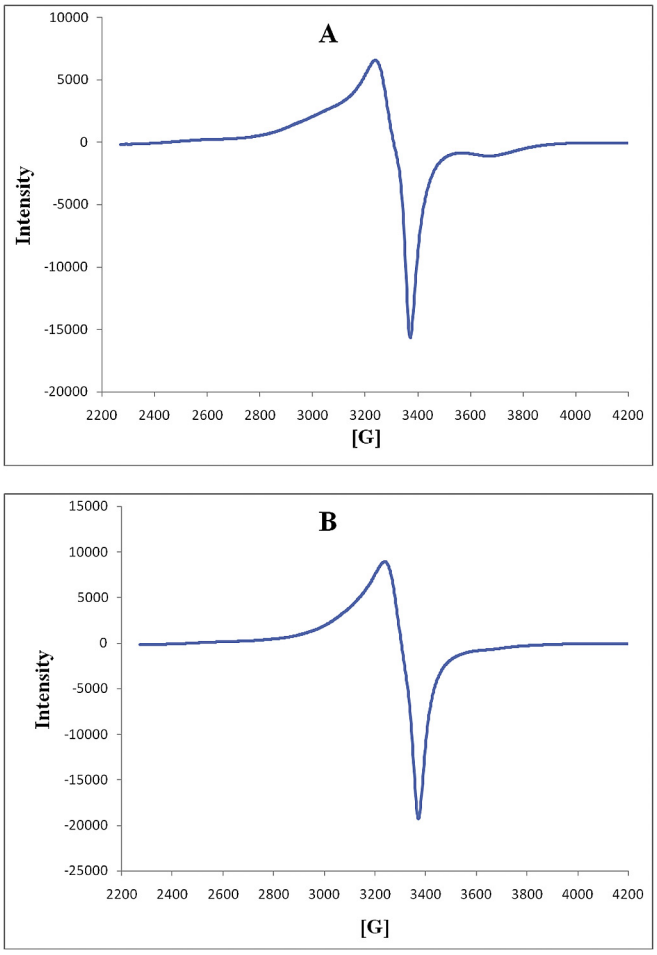

Fig. 4. X-band ESR spectra of the complexes A: $[(L)Cu(SO_4)(H_2O)_2]$ (**3**), and B: $[(L)Cu(Br)_2)]\cdot 0.5H_2O$ (**6**).

thermal analyses. The bands at 1694 and 1643 cm^{-1} assigned to ν(HC═O) and ν(C═O), respectively in the free ligand, were shifted to lower wave number in all complexes, indicating the contribution of the these groups in complex-formation [16–19]. The coordinating modes of anions were deduced from the IR spectra of the current complexes. In complex **1**, the new bands observed at 1498 and 1391 cm^{-1} may be due to $\nu_{as}(COO^-)$ and $\nu_s(COO^-)$, respectively of the acetate group [20]. The difference between the two bands, $\Delta\nu = (\nu_{as}\text{-}\nu_s) = 107\ cm^{-1}$, is consistent with the values cited for the monodentate character of the acetate group [21]. The complexes (**2** and **7**–**9**) showed new bands in the range 1424–1437 cm^{-1}, indicating the ionic nature of the NO_3^- group [22–25]. In complex **3**, the chelating bidentate fashion of SO_4^{2-} group was indicated by the appearance of a new band at 1069 cm^{-1} [26]. In complex **4**, the new bands observed at 1092 and 626 cm^{-1} may be assigned to ν_3 and ν_4 vibrations, respectively of the non-coordinated (ionic) ClO_4^- ion [17,27–30].

The coordinating ability of anions towards the metal ion could be deduced from the linear correlations between the Lewis basicity of anion (DN_X) [31] versus the IR bathochromic shift of the formyl group ($\Delta\nu_{HCO}$ = ν_{HCO} of free ligand - ν_{HCO} of complex), $\Delta\nu_{HCO}.cm^{-1} = 24.53 + 1.626\ DN_X$, r = 0.99, n = 4, except nitrate complex (Fig. 2). The positive slope reveals that the strong interaction of Cu(II) with anion (high basicity, DN_X) enhances the coordination with the chromone ligand (higher extent of bathochromic shift of ν_{HCO}). Moreover, strong Lewis base anions such as chloro, bromo and sulphato display 1:1 (L:M) complexes. However, weak or intermediate anions (perchlorato and acetato) form 2:1 (L:M) complexes. The mixed-ligand complexes showed new bands in the range 1500–1504 cm^{-1}, supporting the coordination of the C═N group of the secondary ligands to the metal ion [22,32,33]. The preceding interpretation is further supported by the appearance of new bands in the ranges 500–538 and 430-470 cm^{-1}, which may be attributed to ν(M-O) and ν(M-N), respectively [24,34–38].

Table 4
ESR data of some copper(II) complexes at room temperature.

Complex	g‖	$g_\perp$	A‖ $\times 10^{-4}$ (cm^{-1})	G	α^2	β^2
$[(L)_2Cu(OAc)_2]\cdot 0.5H_2O$ **(1)**	2.15	2.09	170	1.67	0.7	0.46
$[(L)Cu(SO_4)(H_2O)_2]$ **(3)**	2.14	2.08	211	1.75	0.8	0.38
$[(L)_2Cu(H_2O)_2](ClO_4)_2$ **(4)**	2.16	2.09	230	1.78	0.87	0.4

Table 5
Thermal analysis data of some metal complexes.

Complex	Temperature range (°C)	% Wt. loss Found/(Calc.)	Lost fragment (No. of molecules)
$[(L)_2Cu(OAc)_2]\cdot 0.5H_2O$ (**1**)	37–140	1.66/(1.67)	$0.5H_2O$ (hyd.)
	140–220	22.33/(22.27)	2 AcOH
$[(L)Cu(SO_4)(H_2O)_2]$ (**3**)	110–232	9.58/(9.73)	$2H_2O$ (coord.)
$[(L)CuCl_2(H_2O)_2]\cdot 0.5H_2O$ (**5**)	30–131	2.24/(2.54)	$0.5H_2O$ (hyd.)
	131–208	9.87/(10.18)	$2H_2O$ (coord.)
	208–336	20.64/(20.52)	2HCl
$[(L)CuBr_2)]\cdot 0.5H_2O$ (**6**)	36–145	2.14/(2.21)	$0.5H_2O$ (hyd.)
$[(L)_2Cu(Bipy)](NO_3)_2\cdot 0.5H_2O$ (**9**)	30–132	1.28/(1.1)	$0.5H_2O$ (hyd.)

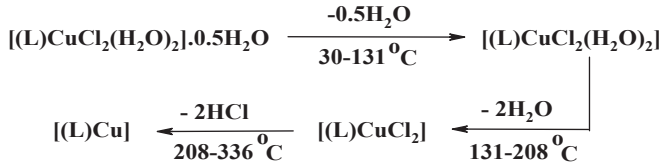

Scheme 2. Thermal degradation pattern of complex (**5**), $[(L)CuCl_2(H_2O)_2]\cdot 0.5H_2O$, in the range of 30–336 °C.

3.2. Conductivity measurements

The molar conductance values of the complexes (Table 3) showed that the complexes can be classified into three categories: (a) 2:1 electrolytes (complexes **2, 4, 8** and **9**), (b) 1:1 electrolytes (complex **7**) and (c) non-electrolytes (complexes **1, 3, 5** and **6**). In case of 1:1 and 2:1 electrolytes, the molar conductance values fall in the expected range [39] indicating that the nitrate or perchlorate anions are situated outside the metal coordination sphere. This is consistent with the weak coordinating ability of nitrate and perchlorate anions. Moreover, infrared spectral data showed the presence of ionic nitrate and perchlorate groups (catioinic complexes) whilst coordinated acetate and sulphate groups (neutral complexes).

3.3. Magnetic measurements and electronic spectra

The magnetic moment values of the complexes (except **2** and **8**) are in the range 1.56–2.15 B.M., which is consistent with one unpaired electron (d^9) [40–42]. However, complexes **2** and **8** have magnetic moments (2.3 B.M.) higher than the calculated value for one unpaired electron, which may be due to spin-orbit coupling [43].

Electronic spectra of the copper(II) complexes were examined for DMF solutions and/or Nujol mulls for sparingly soluble complexes. Comparison of the spectrum of the free ligand with its copper(II) complexes showed the appearance of the bands of the ligand in all complexes with a slight blue or red shift in addition to new bands, which are summarized in Table 3. Fig. 3 represents electronic spectra of some representative complexes.

The electronic spectra of the complexes (**1**–**5**, **7**–**9**) showed two absorption bands in the ranges 423–500 and 615–701 nm, which may be assigned to the $^2B_{1g} \rightarrow {}^2E_g$ and $^2B_{1g} \rightarrow {}^2B_{2g}$ transitions, respectively corresponding to a distorted octahedral geometry [17,32,44,45]. On the other hand, complex **6** showed bands at 510 and 695 nm, which may be assigned to the $^2B_{1g} \rightarrow {}^2A_{1g}$ transition in a square planar geometry. This finding is confirmed by ESR spectral data (*vide infra*) [46,47].

3.4. ESR spectra

ESR spectra of the complexes (**1**, **3**, **4** and **6**) were recorded in the solid state to get further information about the stereochemistry of the complexes. Fig. 4 represents the ESR spectra of complexes **3** and **6**. The spin Hamiltonian parameters of the complexes were calculated and summarized in Table 4. The room temperature solid state ESR spectra of the complexes are quite similar and display an axially *g*-tensor parameters with $g_{\|} > g_{\perp} > 2.0023$. The profiles of the spectra indicate octahedral geometry around the Cu(II) center in complexes **1**, **3** and **4** and square planar for complex **6** [17,23,48–51]. The $g_{\|}$ value is a significant factor for indicating covalent character of M–L bonds [52,53]; for ionic character, $g_{\|} > 2.3$ and for covalent character $g_{\|} < 2.3$. In the present complexes, the $g_{\|}$ values (Table 4) are less than 2.3 indicating considerable covalent character for the Cu-L bond. The values of the exchange interaction parameter term *G*, estimated from the expression $G = (g_{\|} - 2)/(g_{\perp} - 2)$ [54,55], are lower than 4, suggesting copper–copper exchange interactions.

Molecular orbital coefficients, α^2(a measure of the covalency of the in-plane σ-bonding between copper 3d orbital and the ligand orbitals) and β^2 (covalent in-plane π-bonding), were calculated [56]. The lower values of β^2 compared to α^2 indicate that the in-plane π-bonding is more covalent than the in-plane σ-bonding. These results are in consistent with the data obtained previously [30,57–60].

3.5. Thermal analysis

The simultaneous TGA analysis of metal complexes was studied from ambient temperature to 800 °C in nitrogen atmosphere. Moreover, the kinetic and thermodynamic parameters using Coats-Redfern equations have also been calculated. Complexes **1**, **3**, **5**, **6** and **9** were taken as representative examples for this study. The results of thermal analysis (Table 5) of these complexes are found in agreement with elemental analyses.

The first stage of decomposition of the complexes extends up to 145 °C, corresponding to the loss of non-coordinated water

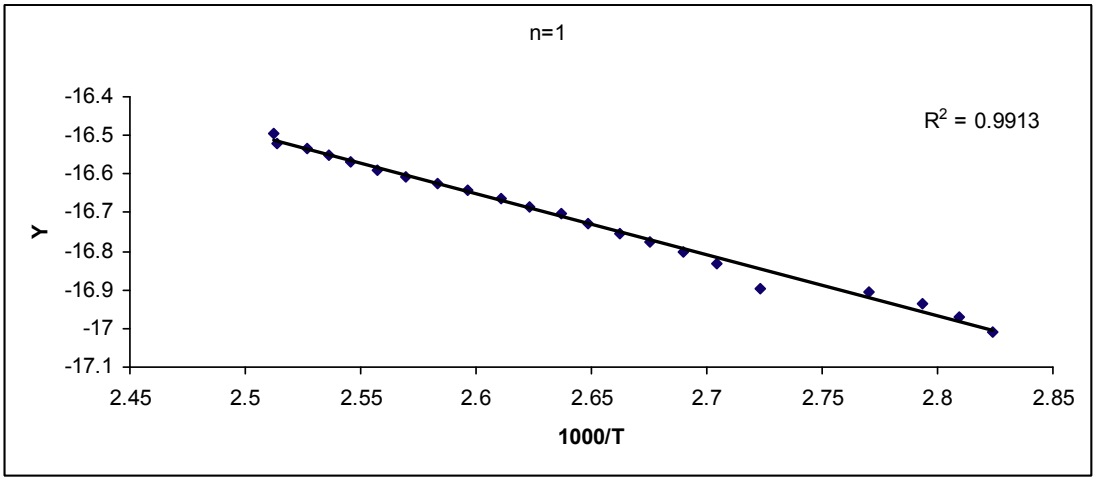

First stage

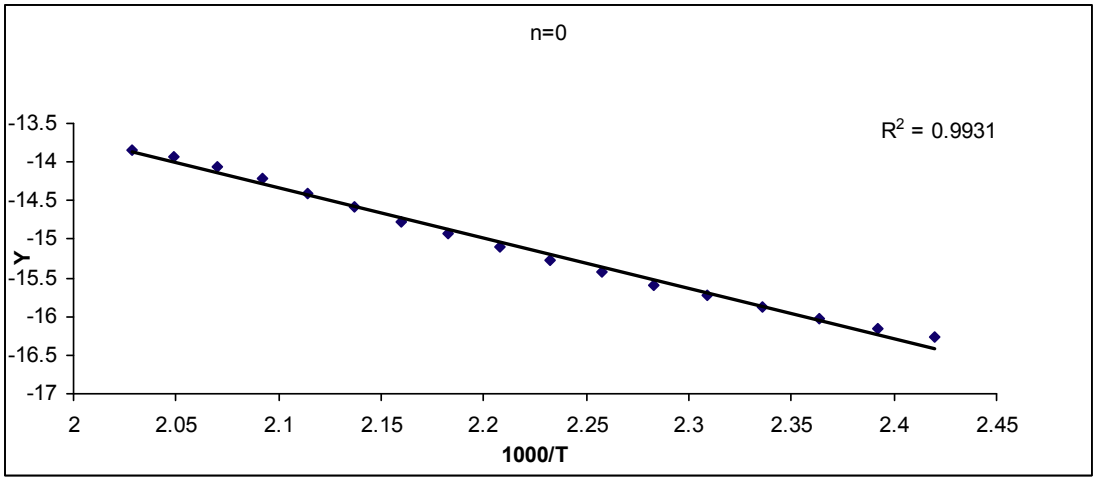

Second stage

Fig. 5. Coats-Redfern plots for $[(L)_2Cu(OAc)_2]\cdot 0.5H_2O$ (**1**), where $Y = \ln[-\ln(1-\alpha)/T^2]$.

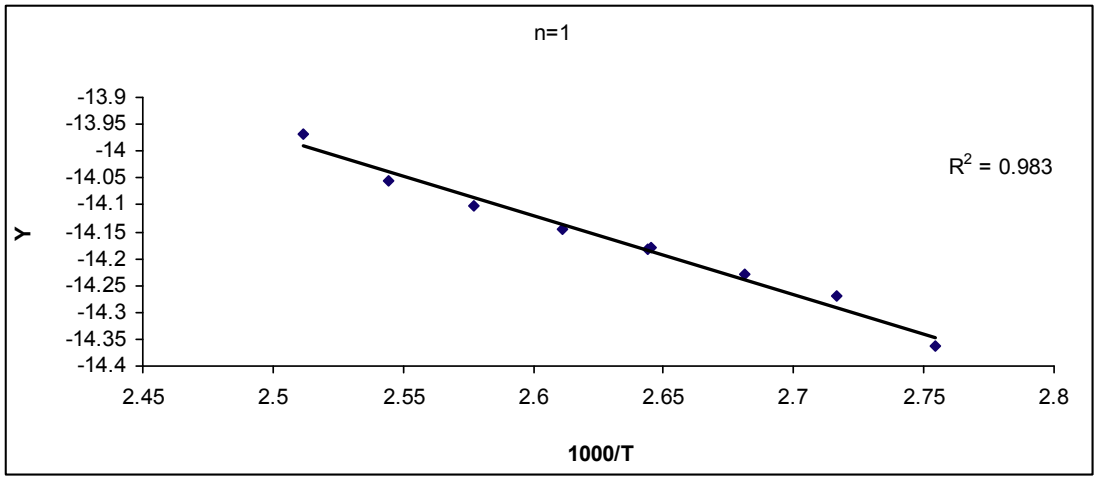

First stage

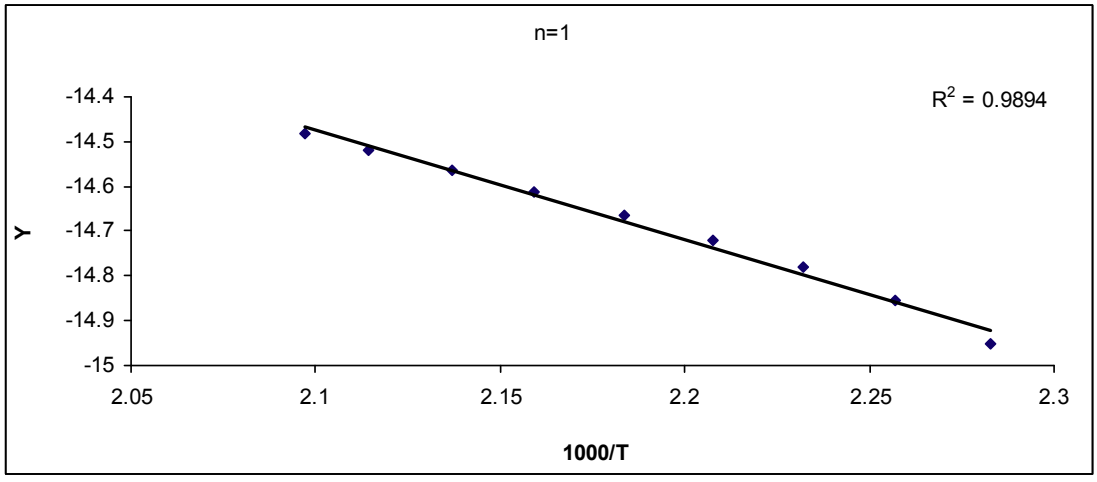

Second stage

Fig. 6. Coats-Redfern plots for $[(L)CuCl_2(H_2O)_2]\cdot 0.5H_2O$ (**5**), where $Y = \ln[-\ln(1-\alpha)/T^2]$.

Table 6
Temperatures of decomposition and the kinetic parameters of complexes.

Complex	Step	n order	T (K)	A (S^{-1})	Δ E (kJ mol^{-1})	ΔH (kJ mol^{-1})	ΔS (kJ mol^{1} K^{-1})	ΔG (kJ mol^{-1})
$[(L)_2Cu(OAc)_2]\cdot 0.5H_2O$	First	1	355	0.069	13.65	10.706	−1.1520	419.67
	Second	0	473	37665	54.58	50.64	−1.044	544.7
$[(L)Cu(SO_4)(H_2O)_2]$	First	1	472	165.8	38.21	34.28	−1.089	548.28
$[(L)CuCl_2(H_2O)_2]\cdot 0.5H_2O$	First	1	360	1.6349	15.326	12.33	−1.1257	417.58
	Second	1	443	12.59	26.089	22.40	−1.110	514.38
$[(L)CuBr_2)]\cdot 0.5H_2O$	First	1	399	115.34	35.12	31.80	−1.091	467.10
$[(L)_2Cu(Bipy)](NO_3)_2\cdot 0.5H_2O$	First	1	362	0.2763	18.056	15.04	−1.1405	430.94

molecules. The second stage of decomposition extends up to 232 °C corresponding to the loss of coordinated water or acetic acid molecules. In case of complex **5**, the third stage of decomposition extends up to 336 °C corresponding to the loss of two HCl molecules. Scheme 2 summarizes the degradation steps of complex **5**.

The kinetic and thermodynamic parameters of the thermal degradation of the complexes namely, activation energy (Ea), enthalpy (ΔH), entropy (ΔS) and free energy changes (ΔG) were calculated using Coats–Redfern method [61]. The Coats–Redfern equations are in the following form:

$$\ln\left[1-(1-\alpha)^{1-n}\Big/(1-n)T^2\right] = \ln(AR/\beta E) - (Ea/R)T \quad \text{for } n\neq 1 \qquad (1)$$

$$\ln\left[-\ln(1-\alpha)\Big/T^2\right] = \ln(AR/\beta E) - (Ea/R)T \quad \text{for } n\neq 1 \qquad (2)$$

where α represents the fraction of sample decomposed at time t, defined by: $\alpha = (w_o - w_t)/(w_o - w_\infty)$, w_o, w_t and w_∞ are the weight of the sample before the degradation, at temperature t °C and after total conversion, respectively. T is the derivative peak temperature. Ea, R, A and β are the heat of the activation, the universal gas constant, pre-exponential factor and heating rate, respectively.

The correlation coefficient, *r*, was computed using the least square method for different values of *n* ($n = 0.33, 0.5, 0.66$ and 1), by plotting the left–hand side of Eqs. (1) or (2) versus 1000/T (Figs. 5 and 6). The *n* value which gave the best fit ($r \approx 1$) was chosen as the order parameter for the decomposition stage of interest. From the intercept and linear slope of such stage, the A and E_a values were determined.

The other kinetic parameters, ΔH^*, ΔS^* and ΔG^* were also calculated by Eyring equation [62]: $\Delta H^* = E_a - RT$, $\Delta S^* = R[\ln(Ah/kT)-1]$ and $\Delta G^* = \Delta H^* - T.\Delta S^*$, where *k* is the Boltzmann's constant and h is the Plank's constant. The following remarks can be pointed out on the kinetic parameters; Table 6. (1) The value of ΔH decreases significantly for the subsequently decomposition stages. (2) The negative values of activation entropies ΔS indicate a more order activated complex than reactant and/or the reaction is slow. (3) The energy of activation (E_a) values decrease on going from one decomposition stage to another for a given complex, indicating that the rate of removal of decomposition increases in the same order.

3.6. Mass spectra

In order to get further information about the molecular formulae of the complexes, mass spectra of complexes **1, 2, 5** and **7**, as representative examples, were carried out. Fig. 7 depicts the mass spectra of complexes **1** and **2**. The mass spectra of the complexes **1, 2, 5** and **7** showed the molecular mass peak with *m/z* 530, 710, 345 and 618, respectively, which are consistent with the formula weights of the anhydrous complexes $[(L)_2Cu(OAc)_2]$ (F. Wt = 529.96), $[(L)_3Cu](NO_3)_2$ (F. Wt = 710.03), $[(L)CuCl_2(H_2O)_2]$ (F. Wt = 344.65) and $[(L)_2Cu(8\text{-HQ})]NO_3$ (F. Wt = 618.02).

In conclusion, based on the elucidation of elemental and

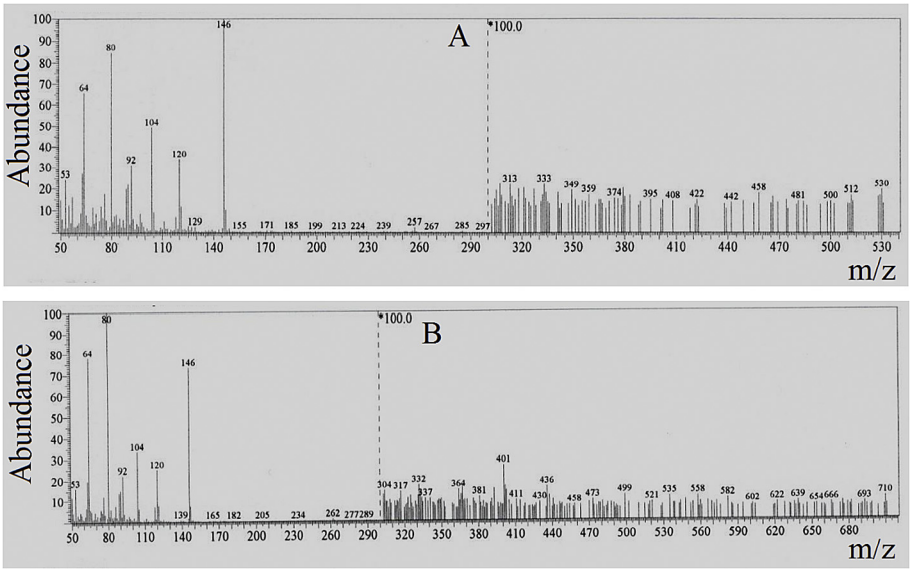

Fig. 7. Mass spectra of the complexes A: $[(L)_2Cu(OAc)_2]\cdot 0.5H_2O$ (**1**) and B: $[(L)_3Cu](NO_3)_2\cdot MeOH$ (**2**).

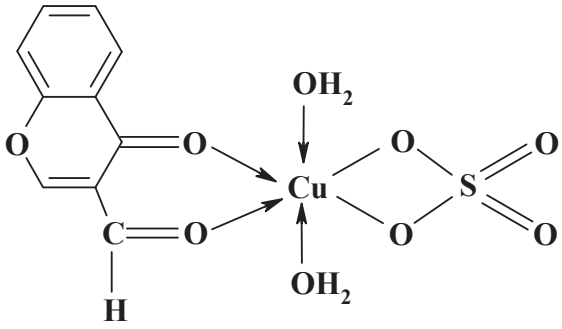

(3)

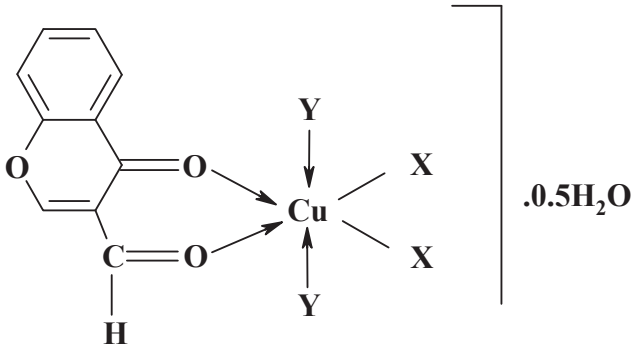

X	Y	Complex
Cl	H_2O	**5**
Br	nil	**6**

Scheme 3. Representative structures of 1:1 (M:L) binary complexes obtained by using SO_4^{2-}, Cl^- and Br^- anions.

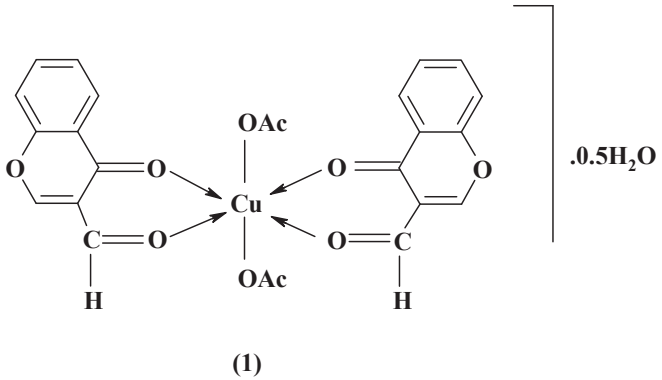

(1)

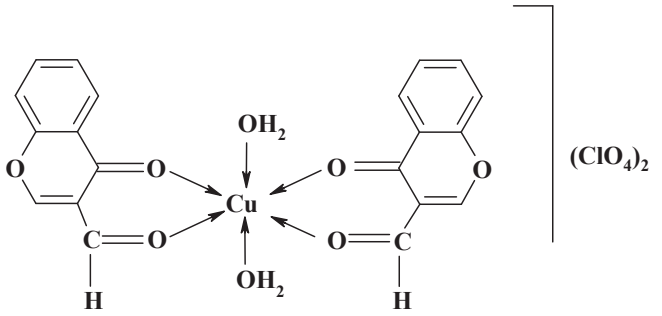

(4)

Scheme 4. Representative structures of 1:2 (M:L) binary complexes obtained by using OAc^- and ClO_4^- anions.

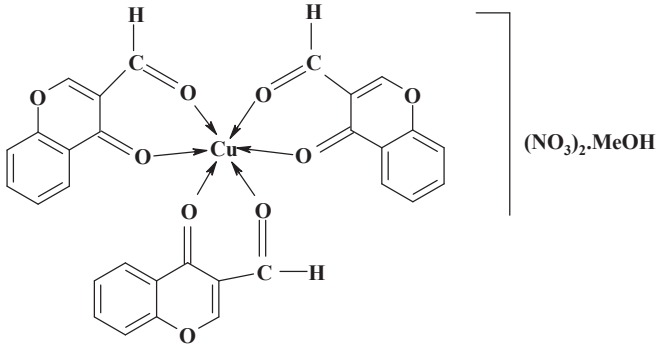

(2)

Scheme 5. Representative structures of the 1:3 (M:L) binary complex obtained by using NO_3^- anion.

thermal analyses and spectral data (infrared, electronic, ESR and mass) as well as conductivity and magnetic susceptibility measurements at room temperature, proposed structures of the metal complexes are represented in Schemes 3–6.

3.7. Molecular orbital calculations

The molecular structures were carried out for the free ligand and its complexes on the basis of the semi-empirical *PM3* level provided by *HyperChem 7.52* software. Geometrical optimization was carried out for the structures of the current compounds, which were elucidated on the basis of spectral, molar conductance, magnetic susceptibility and TGA data. Fig. 8 denotes the optimized structures of complexes **3** and **5** as representative examples and the calculated structural parameters (heat of formation, dipole moment, HOMO and LUMO energies) are listed in Table 7.

It is well established that HOMO accounts for the electron donating ability, while LUMO characterizes the ability to accept electron [63]. Consequently, high LUMO energy value infers that the molecule can easily accept electrons from the occupied orbital of the ligand, indicating strong binding affinity. The linear correlation between the calculated energy of the unocupied molecular orbital (E_{LUMO}) versus the bathochromic shift of the streching frequency of the formyl group ($\Delta\nu_{HCO}$), E_{LUMO}/eV = 3.160−0.069 $\Delta\nu_{HCO}$.cm^{-1}, r = 0.97, n = 6 points, except ClO_4^-, Cl^- and bipy complexes.The negative slope states that the high extent of the bathochromic shift accompanied by decrease of E_{LUMO} as shown in Fig. 9. A comparison between the bond lengths of the ligand and its metal complexes is demonstrated in Table 8. The theoretical data were compared with the experimental data of the antimicrobial activity (*vide infra*).

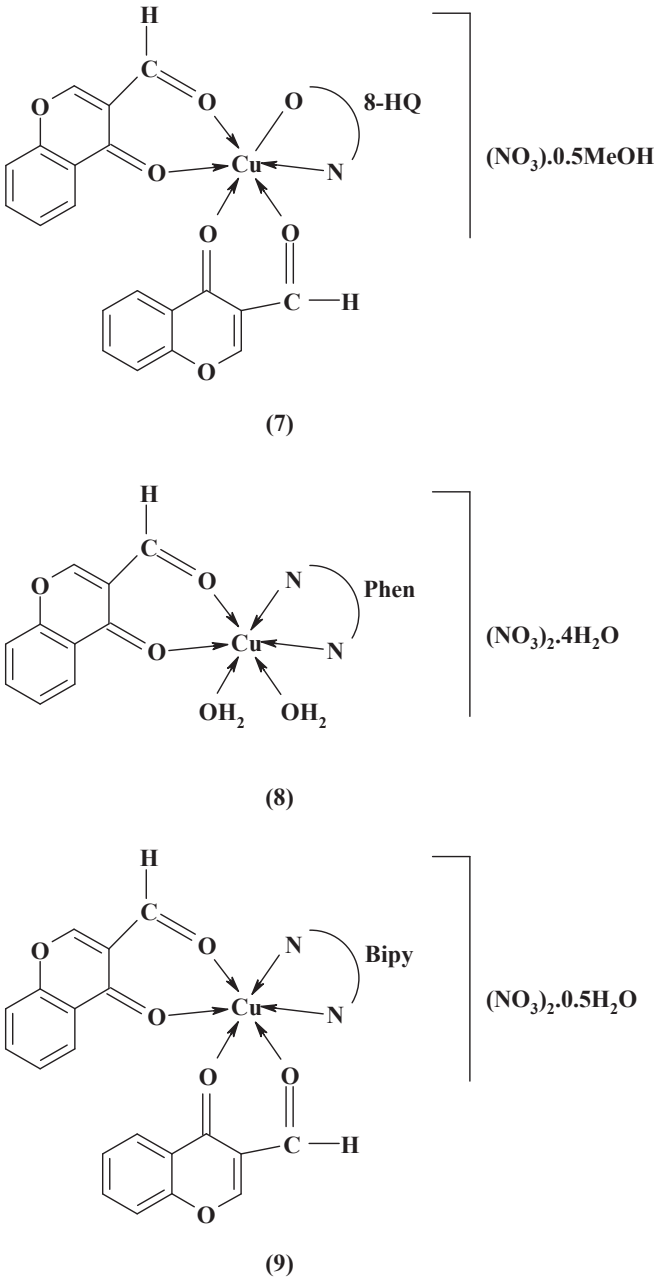

Scheme 6. Representative structures of the ternary complexes.

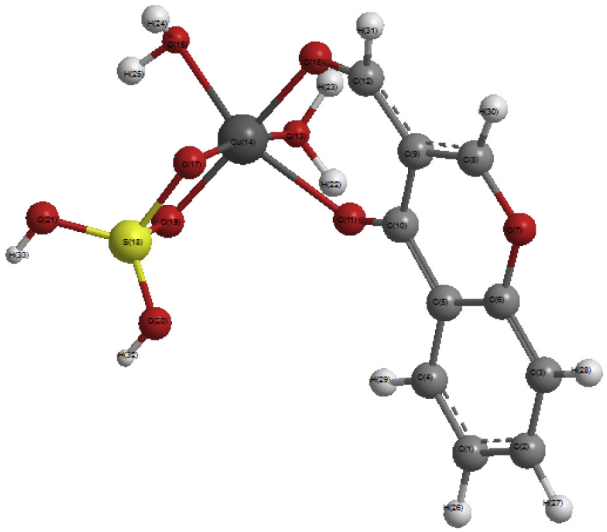

[(L)Cu(SO$_4$)(H$_2$O)$_2$] (**3**)

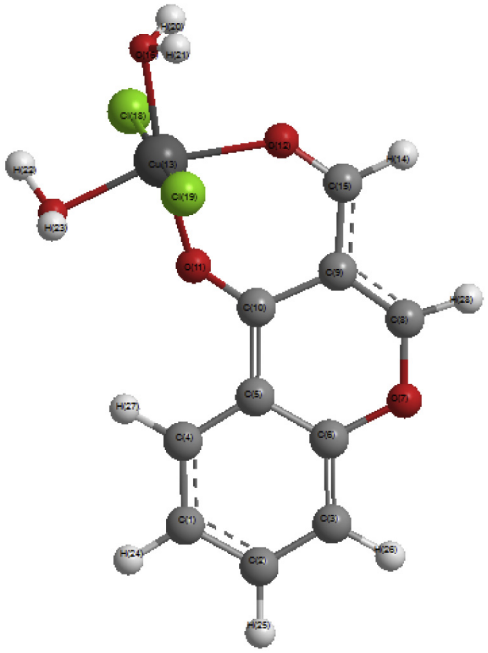

[(L)CuCl$_2$(H$_2$O)$_2$]·0.5H$_2$O (**5**)

Fig. 8. Optimized structures of some representative complexes (**3** and **5**).

3.8. Antimicrobial studies

The free ligand and its Cu(II)-complexes were evaluated for sensitive organisms which are: two strains *Staphylococcus aureus* (*G+1*) and *Bacillus subtilis* (*G+2*) as Gram-positive bacteria, *Escherichia coli* (*G-1*) and *Salmonella typhimurium* (*G-2*) as Gram-negative bacteria, in addition to Yeast: *Candida albicans* (*F1*) and Fungus: *Aspergillus fumigatus* (*F2*) and the results are listed in Table 9. The ligand exhibits intermediate to higher bioactivity against all organisms and its activity is promising toward *Candida albicans (F1)*. The bioactivity of the current complexes varies from lower to higher activity as indicated in Table 9, in some cases, exhibited higher than that of the control and thus the complex may be subjected to further studies. The perchlorate complex **4** displayed the highest antimicrobial activity (except for Gram-positive bacteria) than the other complexes. Furthermore, the mixed complex with 1,10-phenanthroline **8** showed the highest activity towards all of microorganisms used in this study.

It is recognized that different factors such as nature of the chelating agent and its chelating sites, nature of the metal ion, geometrical structure of the complex, solubility and other factors have significant effects on the antibacterial activity of a compound [64]. Electron donicity (*ED*), in particular, is an appropriate theoretical parameter accounting for the extent of Lewis acid-base

Table 7
Molecular orbital parameters of the ligand and its metal complexes on the PM3 level.

Property	Ligand	1	2	3	4	5	6	7	8	9
Total energy (kcal/mol)	−49742	−166989.46	−176257.84	−123498.72	−141826.89	−106696.86	−93345.75	−164046.015	−169903.28	−164450.2
Binding energy (kcal/mol)	−2264	−6067.97	−6618.4013	−3341.9819	−5113.678	−2923.38	−2400.607	−6681.953	−7278.82	−6955.894
Electronic energy (kcal/mol)	−250173	−407897.25	−1569652.5	−748591.125	−1047575.3	−582271.8	−434069.8	−1453268.62	−1611635.75	−1513069.87
Heat of formation (kcal/mol)	−63.83	−352.4859	62.8654	−428.9308	−305.0749	−256.990	−66.2381	−177.6945	−104.246	−123.10062
Dipole moment (D)	4.08	11.49	8.006	7.639	5.771	5.927	14.73	6.227	8.433	6.783
HOMO (eV)	−9.77	−3.745337	−4.050229	−4.034081	−2.66725	−4.414013	−5.50636	−6.9746	−2.531	−2.618603
LUMO (eV)	−0.88	−1.775317	−2.417258	−0.97625	−0.76984	−1.27945	−2.119755	−0.9164	−1.0315	−1.003317
Hydration energy	7.31	−2.56	−0.38	−29.93	−19.68	−18.32	−1.26	−2.66	−2.12	−6.33
Polarizability	17.62	42.57	49.49	20.49	34.55	22.71	22.55	49.22	54.51	51.80

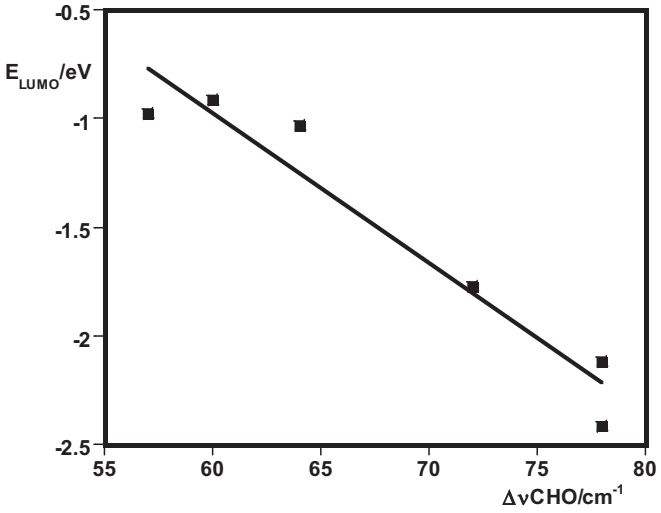

Fig. 9. Relationship of E_{LUMO} versus the extent of the IR bathochromic shift of the formyl group.

interactions between ligand (Lewis base) and Cu(II) (Lewis acid). The higher the *ED* becomes the higher the electron rate flow from ligand to metal ion. *ED* was calculated according to the empirical Eq. (3) by the difference between the total energies of complex (TE_C) and free ligand (TE_L).

$$ED = TE_C - TE_L \quad (3)$$

Correlating the normalized biological activity data in Table 9, "rationalize the measured data to the control value", versus the structural parameters data (Table 7) and spectral data in Table 2 yield the following correlations: *G+2* = 0.734 + 0.024 *ED* kcal/mol), *r* = 0.99, n = 5 points, (Fig. 10); *G-1* = 0.236 + 0.075 *ED* kcal/mol, *r* = 0.99, n = 4 points; *F1* = 0.716 + 0.030 *ED* kcal/mol, *r* = 0.95, n = 4 points and *F2* = 0.504 + 0.070 *ED* (kCal/mol), r = 0.96, n = 4 points. The positive slopes reveal that the increasing of the stability of complex (high value ED) develops the bioactivity of complex against the microrganism.

Furthermore, E_{gap}/eV = 0.734 + 0.024 *G+2*, r = 0.97, n = 5 points, except OAc^-, SO_4^{2-}, 8-HQ and bipy complexes (Fig. 11), E_{gap}/eV = 0.321 + 0.024 *G-2*, r = 0.96 n = 6 points, excpet ClO_4^-, 8-HQ and phen complexes and E_{gap} eV = −0.649 + 0.189 *F2*, r = 0.97 n = 4 points, except OAc^-, NO_3^-, SO_4^{2-}, ClO_4^- and bipy complexes. The positive slopes of the correlations indicate again that increasing E_{gap} that measures stability of the complex, enhances the biological activity against the current micro-organisms.

Likewise, the positive slopes of the linear relationships of the biological activity against *G-1 and G+2* versus the streching frequency $\Delta\nu_{C=O}$ (formyl), yield, *G*-1 = 0.236 + 0.075 $\Delta\nu_{C=O}$ cm^{-1}, *r* = 0.99, n = 4 points except SO_4^{2-}, Cl^-, Br^-, 8-HQ and bipy complexes, and *G*+2 = 0.734 + 0.024 $\nu_{C=O}$ cm^{-1}, *r* = 0.97, n = 5 points except OAc^-, SO_4^{2-}, 8-HQ and bipy complexes. This finding points again to increasing the biological activity with the red shift of $\nu_{C=O}$ (formyl), high bond strength (more binding interaction between the metal ion and formyl group of the ligand).

Additionally, increasing the polarity of the complexes (measured by the values of the dipole moment) leads to increase the biological activity of the complex as indicated from the positive slope of this correlation, dipole moment = 0.734 + 0.0243 *G+2*, *r* = 0.97, n = 5 points except OAc^-, SO_4^{2-}, 8-HQ and bipy complexes.

Table 8
Theoretical calculated bond lengths (Å) of the ligand (L) and its metal complexes on the PM3 level.

	Compound	C=O	C=Oγ pyrone	M-O=C	M-O=C γ	Other bond lengths
	L	1.21	1.22	–	–	–
1	$[(L)_2Cu(OAc)_2]\cdot 0.5H_2O$	1.23	1.25	2.03	1.97	M-OAc 1.86–1.85
2	$[(L)_3Cu](NO_3)_2\cdot MeOH$	1.23	1.24	2.01	2.01	–
3	$[(L)Cu(SO_4)(H_2O)_2]$	1.22	1.26	2.06	1.90	M-OSO_3 1.84
4	$[(L)_2Cu](ClO_4)_2$	1.24	1.26	1.92	1.92	–
5	$[(L)CuCl_2(H_2O)_2]\cdot 0.5H_2O$	1.23	1.25	2.04	1.99	M-Cl 2.23
6	$[(L)CuBr_2)]\cdot 0.5H_2O$	1.23	1.25	1.92	1.92	M-Br 2.39
7	$[(L)_2Cu(8\text{-}HQ)]NO_3\cdot 0.5MeOH$	1.22	1.24	1.98	1.91	M-8HQ 1.90
8	$[(L)Cu(Phen)(H_2O)_2](NO_3)_2\cdot 4H_2O$	1.23	1.24	2.04	2.00	M-Phen 1.93
9	$[(L)_2Cu(Bipy)](NO_3)_2\cdot 0.5H_2O$	1.23	1.24	2.13	2.05	M-Bipy 1.90–1.92

Table 9
Antimicrobial activity of the ligand and its Cu(II) complexes.

Sample	Mean[a] of zone diameter, nearest whole mm.											
	Gram - positive bacteria				Gram - negative bacteria				Yeasts and Fungi[b]			
	Staphylococcus aureus (ATCC 25923)		*Bacillus subtilis* (ATCC 6635)		*Salmonella typhimurium* (ATCC 14028)		*Escherichia coli* (ATCC 25922)		*Candida albicans* (ATCC 10231)		*Aspergillus fumigatus*	
	Concentration											
	1 mg/ml	0.5 mg/ml	1 mg/ml	0.5 mg/ml	1 mg/ml	0.5 mg/ml	1 mg/ml	0.5 mg/ml	1 mg/ml	0.5 mg/ml	1 mg/ml	0.5 mg/ml
L	22 I	19 H	31 H	27 H	29 H	26 H	24 I	20 H	43 H	38 H	25 I	20 H
$[(L)_2Cu(OAc)_2]\cdot 0.5H_2O$ (**1**)	22 I	17 I	17 I	13 I	14 I	12 I	15 I	13 I	37 H	34 H	28 H	25 H
$[(L)_3Cu](NO_3)_2\cdot MeOH$ (**2**)	20 I	17 I	28 H	24 H	17 I	15 I	15 I	13 I	34 H	31 H	24 I	20 H
$[(L)Cu(SO_4)(H_2O)_2]$ (**3**)	13 I	10 I	32 H	27 H	9 L	7 L	15 I	13 I	36 H	30 H	30 H	26 H
$[(L)_2Cu(H_2O)_2](ClO_4)_2$ (**4**)	21 I	19 H	30 H	26 H	21 I	17 I	21 I	18 I	39 H	36 H	34 H	30 H
$[(L)CuCl_2(H_2O)_2]\cdot 0.5H_2O$ (**5**)	15 I	13 I	31 H	26 H	10 L	9 L	17 I	14 I	32 H	28 H	20 I	16 I
$[(L)CuBr_2)]\cdot 0.5H_2O$ (**6**)	14 I	12 I	32 H	29 H	15 I	13 I	18 I	16 I	32 H	28 H	23 I	19 H
$[(L)_2Cu(8\text{-HQ})]NO_3\cdot 0.5MeOH$ (**7**)	9 L	7 L	26 H	23 H	10 L	8 L	–	–	33 H	29 H	30 H	27 H
$[(L)Cu(Phen)(H_2O)_2](NO_3)_2\cdot 4H_2O$ (**8**)	42 H	37 H	33 H	28 H	33 H	29 H	40 H	37 H	39 H	36 H	41 H	38 H
$[(L)_2Cu(Bipy)](NO_3)_2\cdot 0.5H_2O$ (**9**)	25 H	22 H	32 H	28 H	17 I	14 I	22 I	19 H	36 H	34 H	25 H	20 H
Control[c]	35	26	35	25	36	28	38	27	35	28	37	26

–=No effect.
L: Low activity = Mean of zone diameter ≤1/3 of mean zone diameter of control.
I: Intermediate activity = Mean of zone diameter ≤2/3 of mean zone diameter of control.
H: High activity = Mean of zone diameter >2/3 of mean zone diameter of control.
[a] Calculated from 3 values.
[b] identified on the basis of routine cultural, morphological and microscopical characteristics.
[c] Chloramphenicol in the case of Gram-positive bacteria, cephalothin in the case of Gram-negative bacteria and cycloheximide in the case of fungi.

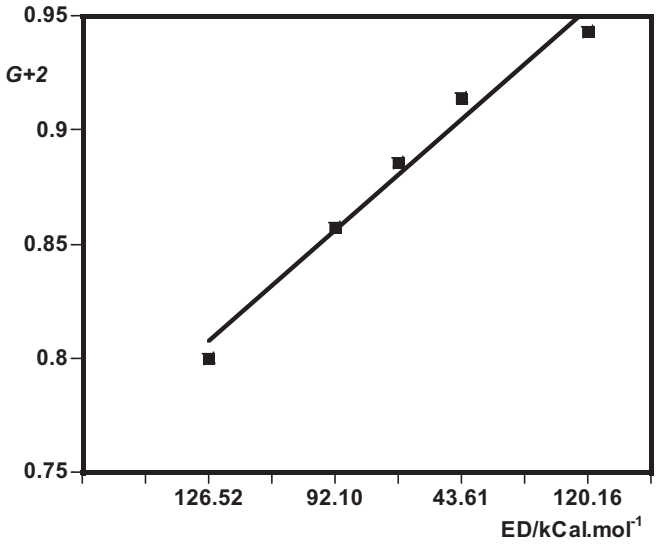

Fig. 10. Correlation between the electrondonicity (ED) and the normalized bioactivity toward *Bacillus subtilis* (*G+2*) as Gram-positive bacteria.

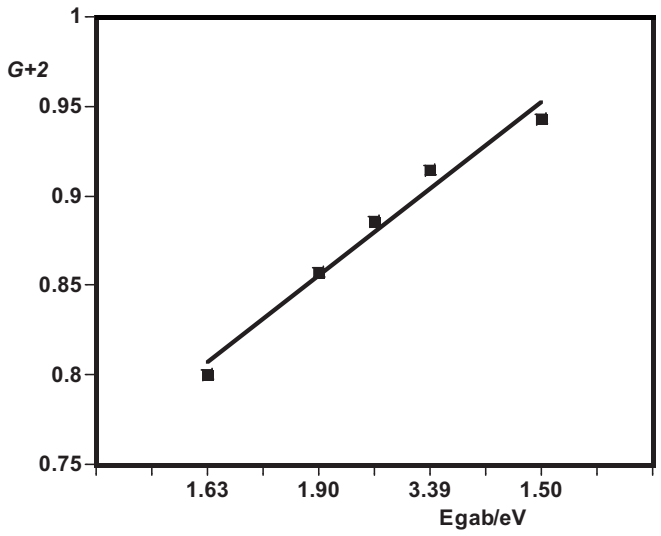

Fig. 11. Linear correlation of Egab versus the normalized bioactivity of compounds toward the Gram positive bacteria (*G+2*).

4. Conclusion

Reactions of 3-formylchromone as a primary ligand (L) with different copper(II) salts afforded neutral and cationic mononuclear complexes with molar ratios: 1:1, 1:2 and 1:3; M:L. Also, ternary complexes were synthesized with molar ratios: 1:2:1 and 1:1:1; M:L:L′ by using various secondary ligands (L′). The spectroscopic data showed that the ligand acts as a neutral bidentate ligand and the metal complexes exhibited octahedral and square planar geometrical arrangements. The ESR spin Hamiltonian parameters of some complexes were calculated and discussed. Kinetic parameters of the thermal decomposition stages have been evaluated using Coats–Redfern equations. Molecular parameters of the ligand and its metal complexes have been calculated and correlated with the experimental data; the changes of bond lengths are linearly correlated with IR data. The ligand and some complexes showed variable antimicrobial activity towards selected kinds of Gram–-positive bacteria, Gram–negative bacteria, yeast and fungus.

References

[1] V. Barve, F. Ahmed, S. Adsule, S. Banerjee, S. Kulkarni, P. Katiyar, C.E. Anson, A.K. Powell, S. Padhye, F.H. Sarkar, J. Med. Chem. 49 (2006) 3800–3808.
[2] C. Marzano, M. Pellei, F. Tisato, C. Santini, Anti Cancer Agents Med. Chem. 9 (2009) 185–211.
[3] M.-H. Pan, C.-S. Lai, C.-T. Ho, Food Funct. 1 (2010) 15–31.
[4] D.P. Ilboudo, N. Basilico, S. Parapini, Y. Corbett, S. D'Alessandro, M. Dell'Agli, P. Coghi, S.D. Karou, R. Sawadogo, C. Gnoula, J. Simpore, J.-B. Nikiema, D. Monti, E. Bosisio, D. Taramelli, J. Ethnopharmacol. 148 (2013) 763–769.
[5] M.C. Patel, N.G. Nilesh, D.P. Rajani, Der Pharma Chem. 3 (2011) 422–432.

[6] H.K. Sandhar, B. Kumar, S. Prasher, P. Tiwari, M. Salhan, P. Sharma, Int. Pharm. Sci. 1 (2011) 25–41.
[7] A. Gomes, M. Freitas, E. Fernandes, J.L.F.C. Lima, Mini Rev. Med. Chem. 10 (2010) 1–7.
[8] S. Khadem, R.J. Marles, Molecules 17 (2012) 191–206.
[9] (a) S. Tabassum, A. Asim, F. Arjmand, M. Afzal, V. Bagchi, Eur. J. Med. Chem. 58 (2012) 308–316;
(b) J. Ravichandran, P. Gurumoorthy, M.A.I. Musthafa, A.K. Rahiman, Spectrochim. Acta A 133 (2014) 785–793.
[10] (a) C. Dendrinou-Samara, G. Psomas, C.P. Raptopoulou, D.P. Kessis-Soglou, J. Inorg. Biochem. 83 (2001) 7–16;
(b) G. Psomas, C.P. Raptopoulou, L. Iordanidis, C. Dendrinou-Samara, V. Tangoulis, D.P. Kessissoglou, Inorg. Chem. 39 (2000) 3042–3048.
[11] F.E. Mabbs, D.I. Machin, Magnetism and Transition Metal Complexes, Chapman and Hall, London, 1973.
[12] A. Nohara, T. Umetani, Y. Sanno, Tetrahedron 30 (1974) 3553–3561.
[13] HyperChem Verion 7.5, Hypercube, Inc, 2003.
[14] A.U. Rahman, M.I. Choudhary, W.J. Thomsen, Bioassay Techniques for Drug Development, Harwood Academic Publishers, The Netherlands, 2001.
[15] K.M. Khan, Z.S. Saify, A.K. Zeesha, M. Ahmed, M. Saeed, M. Schick, H.J. Kohlbau, W. Voelter, Arzneim. Forsch. 50 (2000) 915–922.
[16] A. Dziewulska-Kulaczkowska, J. Therm. Anal. Calorim. 101 (2010) 1019–1026.
[17] M. Shebl, M.A. Ibrahim, S.M.E. Khalil, S.L. Stefan, H. Habib, Spectrochim. Acta A 115 (2013) 399–408.
[18] D.-C. Ilies, E. Pahontu, S. Shova, R. Georgescu, N. Stanica, R. Olar, A. Gulea, T. Rosu, Polyhedron 81 (2014) 123–131.
[19] Y. Li, Z. Yang, J. Coord. Chem. 63 (2010) 1960–1968.
[20] M. Shebl, S.M.E. Khalil, S.A. Ahmed, H.A.A. Medien, J. Mol. Struct. 980 (2010) 39–50.
[21] S.M.E. Khalil, M. Shebl, F.S. Al-Gohani, Acta Chim. Slov. 57 (2010) 716–725.
[22] M. Shebl, S.M.E. Khalil, Monatsh Chem. 146 (2015) 15–33.
[23] M. Shebl, M.A. El-ghamry, S.M.E. Khalil, M.A.A. Kishk, Spectrochim. Acta A 126 (2014) 232–241.
[24] M. Shebl, J. Coord. Chem. 62 (2009) 3217–3231.
[25] M. Shebl, M. Saif, A.I. Nabeel, R. Shokry, J. Mol. Struct. 1118 (2016) 335–343.
[26] K. Nakamoto, Infrared and Raman Spectra of Inorganic and Coordination Compounds, fifth ed., John Wiley and Sons, New York, 1997.
[27] H.S. Seleem, B.A. El-Shetary, S.M.E. Khalil, M. Mostafa, M. Shebl, J. Coord. Chem. 58 (2005) 479–493.
[28] N.T. Madhu, P.K. Radhakrichnan, Synth. React. Inorg. Met. Org. Chem. 31 (2001) 315–330.
[29] A. Taha, Spectrochim. Acta A 59 (2003) 1611–1620.
[30] O.M.I. Adly, Spectrochim. Acta A 95 (2012) 483–490.
[31] W. Linert, A. Taha, J. Chem. Soc. Dalton Trans. (1994) 1091–1095.
[32] M. Shebl, S.M.E. Khalil, A. Taha, M.A.N. Mahdi, Spectrochim. Acta A 113 (2013) 356–366.
[33] H.S. Seleem, A.A. Emara, M. Shebl, J. Coord. Chem. 58 (2005) 1003–1019.
[34] M. Shebl, Spectrochim. Acta A 70 (2008) 850–859.
[35] M. Shebl, H.S. Seleem, B.A. El-Shetary, Spectrochim. Acta A 75 (2010) 428–436.
[36] S.M.E. Khalil, H.S. Seleem, B.A. El-Shetary, M. Shebl, J. Coord. Chem. 55 (2002) 883–899.
[37] M. Shebl, S.M.E. Khalil, A. Taha, M.A.N. Mahdi, J. Mol. Struct. 1027 (2012) 140–149.
[38] H.S. Seleem, B.A. El-Shetary, M. Shebl, Heteroat. Chem. 18 (2007) 100–107.
[39] W.J. Geary, Coord. Chem. Rev. 7 (1971) 81–112.
[40] A. Taha, O.M.I. Adly, M. Shebl, Spectrochim. Acta A 140 (2015) 74–84.
[41] M. Shebl, Spectrochim. Acta A 73 (2009) 313–323.
[42] M. Shebl, Spectrochim. Acta A 117 (2014) 127–137.
[43] G.A.A. Al-Hazmi, M.S. El-Shahawi, I.M. Gabr, A.A. El-Asmy, J. Coord. Chem. 58 (2005) 713–733.
[44] T.A. Yousef, G.M. Abu El-Reash, M. Al-Jahdali, E.R. El-Rakhawy, Spectrochim. Acta A 129 (2014) 163–172.
[45] M.M. Mashaly, A.T. Ramadan, B.A. El-Shetary, A.K. Dawoud, Synth. React. Inorg. Met. Org. Chem. 34 (2004) 1319–1348.
[46] M.M. Abd-Elzaher, S.A. Moustafa, A.A. Labib, M.M. Ali, Monatsh Chem. 141 (2010) 387–393.
[47] K.M. Raj, B. Vivekanand, G.Y. Nagesh, B.H.M. Mruthyunjayaswamy, J. Mol. Struct. 1059 (2014) 280–293.
[48] M. Shebl, S.M.E. Khalil, F.S. Al-Gohani, J. Mol. Struct. 980 (2010) 78–87.
[49] O.M.I. Adly, Spectrochim. Acta A 79 (2011) 1295–1303.
[50] M. Shebl, J. Coord. Chem. 69 (2016) 199–214.
[51] M. Shebl, J. Mol. Struct. 1128 (2017) 79–93.
[52] J.P. Jasinski, J.R. Bianchani, J. Cuva, F.A. El-Said, A.A. El-Asmy, D.X. West, Z. Anorg. Allg. Chem. 629 (2003) 202–206.
[53] A.A. Abou-Hussen, N.M. El-Metwally, E.M. Saad, A.A. El-Asmy, J. Coord. Chem. 58 (2005) 1735–1749.
[54] B.J. Hathaway, D.E. Billing, Coord. Chem. Rev. 5 (1970) 143–207.
[55] B.J. Hathaway, Struct. Bond. Berl. 57 (1984) 55–118.
[56] C.J. Carrano, C.M. Nunn, R. Quan, J.A. Bonadies, V.L. Pecoraro, Inorg. Chem. 29 (1990) 944–951.
[57] N.M. El-Metwally, I.M. Gabr, A.M. Shallaby, A.A. El-Asmy, J. Coord. Chem. 58 (2005) 1145–1159.
[58] K.S. Abu-Melha, N.M. El-Metwally, Spectrochim. Acta A 70 (2008) 277–283.
[59] B. Jeragh, A.A. El-Asmy, Spectrochim. Acta A 129 (2014) 307–313.
[60] G.M. Abu El-Reash, O.A. El-Gammal, S.E. Ghazy, A.H. Radwan, Spectrochim. Acta A 104 (2013) 26–34.
[61] A.W. Coats, J.P. Redfern, Nature 201 (1964) 68–69.
[62] A.A. Forst, R.G. Pearson, Kinetics and Mechanisms, Wiley, New York, 1961.
[63] O.M.I. Adly, A. Taha, S.A. Fahmy, J. Mol. Struct. 1083 (2015) 450–459.
[64] B. Murukan, K. Mohanan, J. Enz. Inhib. Med. Chem. 22 (2007) 65–70.